13th Int. Particle Acc. Conf. IPAC2022, Bangkok, Thailand JACoW Publishing
ISBN: 978-3-95450-227-1 ISSN: 2673-5490 doi:10.18429/JACoW-IPAC2022-WEPOST007

CENTRE-OF-MASS ENERGY IN FCC-ee

J. Keintzel*, A. Blondel, D. Shatilov†, T.H.B. Persson, R. Tomás, F. Zimmermann
CERN, Geneva 23, Switzerland

Abstract

The Future Circular electron-positron Collider (FCC-ee) is designed for high precision particle physics experiments. This demands a precise knowledge of the beam energies, obtained by resonant depolarization, and from which the center-of-mass energy and possible boosts at all interaction points are then determined. At the highest beam energy mode of 182.5 GeV, the energy loss due to synchrotron radiation is about 10 GeV per revolution. Hence, not only the location of the RF cavities, but also a precise control of the optics and understanding of beam dynamics, are crucial. In the studies presented here, different possible locations of the RF-cavities are considered, when calculating the beam energies over the machine circumference, including energy losses from crossing angles, a non-homogeneous dipole distribution, and an estimate of the beamstrahlung effect at the collision point.

INTRODUCTION

The Large Hadron Collider (LHC) [1] with 27 km circumference is presently the world's largest particle collider and has reached an instantaneous luminosity of about 2×10^{34} cm^{-2}s^{-1}. Its luminosity upgrade, the High Luminosity LHC (HL-LHC) [2] aiming at levelling the luminosity around 5×10^{34} cm^{-2}s^{-1}, will be commissioned in 2029 and is planned to be operating until the 2040s.

Following on from the HL-LHC, a sequence of one possible future lepton and one hadron collider is studied within the framework of the Future Circular Collider (FCC) Feasibility Study, launched by CERN Council in 2021. The FCC integrated project [3] foresees first the construction of an approximately 100 km tunnel incorporating the lepton collider FCC-ee [4]. In a second stage this is followed by a hadron collider, FCC-hh [5]. The FCC-ee is an electroweak, Higgs and top factory, and is set to operate at four distinct energy stages of 45.6, 80, 120 and 170-185.5 GeV, allowing for precision measurements of the Z-, W-, and Higgs-bosons, and the top quark, respectively.

One major change with respect to the CDR design with 12 insertion regions and 2 interaction points (IPs), is that the present baseline features a 4-fold symmetry and 4-fold super-periodicity, and foresees only 8 insertion regions and surface sites (PA, PB, PD, PF, PG, PH, PJ, PL) connected by arcs, with 4 IPs (PA, PD, PG, PJ), and a total circumference of 91 km [6]. A schematic layout of the current FCC-ee layout is shown in Fig. 1. The lepton bunches are injected from the booster at nominal energy into the main rings (top-up injection). RF-cavities are installed in the collider straight sections without an IP, and are compensating for all energy losses, primarily from synchrotron radiation (SR), but also from beamstrahlung and others. For example, at the top-energy about 5 % of the beam energy is lost within one revolution due to SR. Recent preliminary civil engineering studies [7] suggest that PH and PL are the most favorable ones for hosting an RF-system, with PF possibly another, more difficult option. For the data taking around the Z-pole and the W-pair threshold, only one RF-section is used, providing almost equal centre-of-mass (ECM) energies in all interaction points. At $t\bar{t}$ threshold, two RF-sections are necessary, and thus different RF configurations are considered in this work.

Since the FCC-ee is designed for high-precision physics experiments, the exact knowledge of the ECM and the collision energy boost at all interaction points is demanded. Various factors impact the ECM, such as the placement and number of the RF-sections, energy losses, non-zero dispersion, chromatic β-functions, optics errors, orbit offsets, or beam-beam effects [8]. First results of the ECM and the boosts at all interaction points for the newest FCC-ee lattices are presented here, taking into account SR and beamstrahlung losses. Other contributions are not considered and will need to be evaluated carefully in future studies.

The simulations presented in the following are performed for the Z- and the $t\bar{t}$-lattices. At $t\bar{t}$ the beam energy is about 3 times higher than for the initial stage, implying a significant energy loss per turn due to SR. Operation with transversely polarised pilot bunches for precise (10-100 keV) beam energy calibration, using the technique of resonant depolarisation, is envisaged for Z-pole and W-pair operation. At

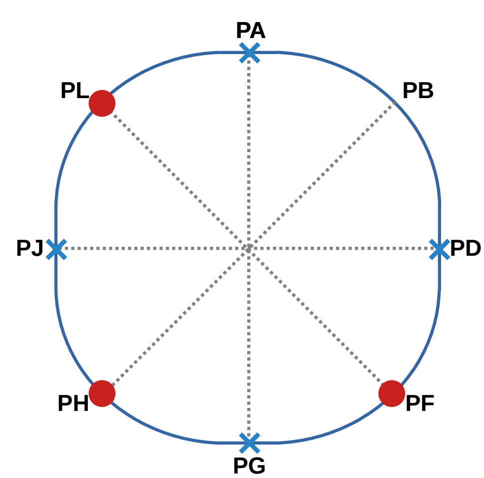

Figure 1: Schematic FCC-ee layout with eight insertion regions. The four IPs are marked with a blue cross. Points suitable to host a RF-system are marked with a red dot.

* jacqueline.keintzel@cern.ch
† on leave from BINP, Novosibirsk, Russia

ISBN: 978-3-95450-227-1 ISSN: 2673-5490 doi:10.18429/JACoW-IPAC2022-WEPOST007

higher energies the ECM energy will be obtained directly from the experiments using $e^+e^- \to Z\gamma$ events with a sufficient precision of a few MeV [8]. Selected FCC-ee beam parameters are compiled in Table 1, further information can be found in [4, 9].

Table 1: Selected FCC-ee Beam Parameters

	Z	$t\bar{t}$
Beam energy [GeV]	45.6	182.5
Full crossing angle [mrad]	30	30
Radiation losses/turn [GeV]	0.04	10
Beamstrahlung/beam/IP [MeV] [1]	0.31	14
RF Voltage [GV]	0.1	5 + 6.7
RF Frequency [MHz]	400	400 + 800

[1] Approximate values, estimated using beam parameters from [6].

SYNCHROTRON RADIATION LOSSES

Charged particles traveling through a guiding magnet loose energy, which is known as SR. The average energy loss for a particle through a dipole with bending radius ρ is given in the literature, e.g. [10], by

$$\Delta E\,[\mathrm{eV}] = \frac{2}{3}\frac{q_0}{4\pi\epsilon_0}\beta_{\mathrm{rel}}^3\gamma_{\mathrm{rel}}^4 \int \frac{1}{\rho^2}\,\mathrm{d}s \qquad (1)$$

with the relativistic factors β_{rel} and γ_{rel}, the unit charge q_0 and the vacuum permittivity ϵ_0. SR is implemented in MAD-X [11] as an extension, which takes into account normal and skew dipole, quadrupole and sextupole fields, together with the orbit at the start and the end of the element [12]. MAD-X also allows for tapering, where the element strengths are reduced according to the radiation losses and thus reducing closed orbit distortions [13]. Thus, tapering reduces the losses from radiation since the dipole strength decreases synchronously to the lost energy. In the present FCC-ee optics all dipole strengths are adjusted individually, resulting in a closed orbit distortion in the order of a few nm [14]. SR losses depend on the local beam energy, which is updated in the MAD-X twiss-module twice for each element. However, the energy used to calculate the radiation losses remains unchanged and is equal to the one corresponding to the nominal beam energy. The losses are, hence, over-estimated for energies lower than the nominal one and vice versa. Over the whole circumference, however, the effect on the total losses is negligibly small. Nevertheless, it is presently investigated in the MAD-X implementation.

BEAMSTRAHLUNG

Particles from two colliding bunches experience the electromagnetic field of the respective opposing bunch, which leads to particular SR emitted during the collision, which is called beamstrahlung. In first approximation, for circular colliders, the beamstrahlung does not change the mean of the energy distribution for colliding particles at the IP. However, photon emissions at the collision point occurring over numerous turns lead to an increased energy spread and bunch length [8, 15]. The energy loss from beamstrahlung can be evaluated using Lifetrac [16], a Monte-Carlo simulation tool for quasi-strong-strong beam-beam simulations. Using few input parameters such as the beam energies, the bunch population, the crossing angle, the bunch length and the emittances, it is possible to compute the energy loss at the interaction point per IP. At the Z- and the $t\bar{t}$-pole the energy loss from beamstrahlung per IP and beam is approximately 0.31 MeV and 14 MeV, respectively, which is also given in Table 1. We model the effect of beamstrahlung by a RF-cavity with a constant energy loss at the four IPs. Analytical descriptions to estimate beamstrahlung have recently been published [17, 18], allowing to evaluate the approximate losses by numerical integration. It is planned to implement such analytical formalism in form of a beamstrahlung element in the code MAD-X, to allow estimating losses dynamically, e.g. in the matching module.

ECM AND BOOSTS

The beam energies are calculated using MAD-X, including SR losses and tapering. If beamstrahlung losses are included, a constant energy loss is assumed in all IPs. Dedicated RF-matching is performed to minimize the differences between the two beams, while keeping the average beam energy over all lattice elements at 45.6 and 182.5 GeV, respectively for the Z- and the $t\bar{t}$-lattice. With the beam energies for the positron and the electron beam, E_+ and E_-, the ECM is calculated by

$$\mathrm{ECM} = 2\sqrt{(E_+E_-)}\cos(\theta/2)\,, \qquad (2)$$

considering also the crossing angle at the IP, θ. ΔECM is the absolute difference with respect to twice the average beam energy, i.e. 91.2 and 365 GeV, respectively. The boost is here defined as $E_+ - E_-$.

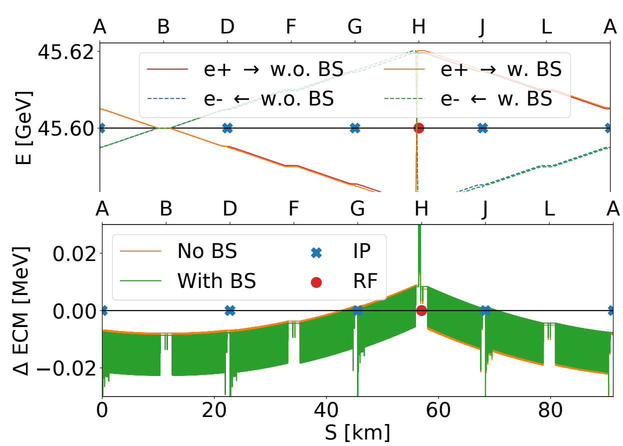

Figure 2: Beam energies (top) and ECM (bottom) at the Z-pole with and without beamstrahlung (BS) at the IPs with a RF-section in PH.

ISBN: 978-3-95450-227-1 ISSN: 2673-5490 doi:10.18429/JACoW-IPAC2022-WEPOST007

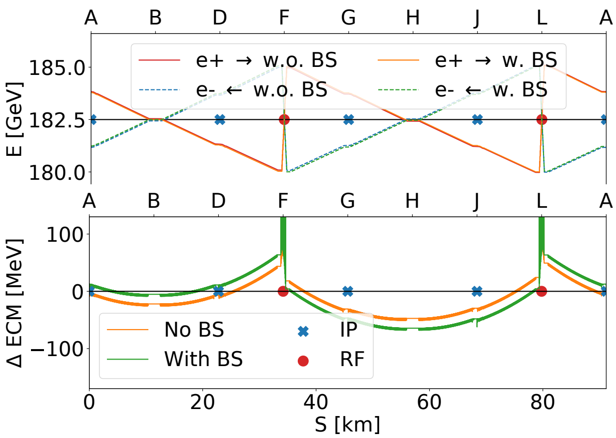

Figure 3: Beam energies (top) and ECM (bottom) at the tt̄-mode with and without beamstrahlung at the IPs for symmetrically placed RF-sections in PL and PF.

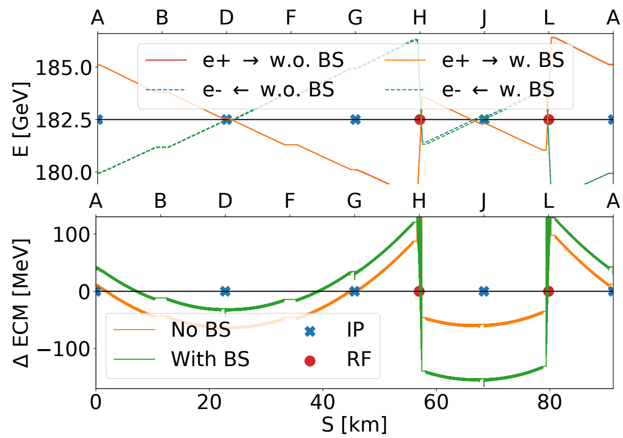

Figure 4: Beam energies (top) and ECM (bottom) at the tt̄-mode with and without beamstrahlung at the IPs for asymmetrically placed RF-sections in PL and PH.

Z-pole: The present design foresees one RF-section, placed here in PH, with 0.1 GV and 400 MHz and thus both beams are accelerated there. The total emitted SR per revolution is about 40 MeV, 0.09 % of the nominal beam energy. Since the beams are travelling in opposite direction, using one RF-section leads to an almost identical ECM at all four IPs, even if beamstrahlung losses are included, as seen in Fig. 2. The absolute difference with respect to twice the beam energy is in the order of a few keV. The boosts are roughly ±10 MeV (PA and PD) and ±30 MeV (PJ and PG). Interestingly, the absolute sum of the boost are almost identical to the losses caused by SR and beamstrahlung.

tt̄-mode: Two RF-sections are required for the tt̄-mode. One 6.7 GV with 800 MHz is assumed to be installed in PL. The location of the second RF-section with a 5 GV, 400 MHz is either in PF, and thus symmetrically placed four arcs later, or asymmetrically in PH (see also Fig. 1). For the symmetric placement option the energy difference between the maximum and the minimum beam energy for each beam is 5.00 GeV, which is equivalent to the losses over over half a revolution. Although the impact of beamstrahlung losses are small compared to SR, they enhance the difference in ECM at the IPs, as seen in Fig. 3. Combined with not identical RF-cavities, the ECM at the IPs is shifted with respect to 365 GeV by approximately 11 MeV (PA and PD) or −47 MeV (PG and PJ). The boosts are about 2.6 GeV (PA and PG) and −2.5 GeV (PD and PJ). With a placement of the RF-sections in PH and PL the difference of the maximum and minimum is larger and about 7.56 GeV, resulting from beams emitting SR over up to 6 arcs before compensation. This placement enhances the asymmetry of the energy loss for both beams, and by including beamstrahlung, the differences in ECM are more severe and result in 43 MeV, −30 MeV, 34 MeV, and −150 MeV, respectively, for PA, PD, PG and PJ, as shown in Fig. 4. The boosts are 5.2 GeV, 0.2 GeV, −4.9 GeV, and −0.2 GeV, respectively. Although asymmetrically placed RF-sections would introduce an initial asymmetry, it is presently presumed that these differences between the four IPs are small enough for physics requirements [19]. Recent studies [20] also investigate in a less challenging 2-cell cavity design with a 2.48 GV, 400 MHz RF-system in PL together with a 9.19 GV 800 MHz one in PH, which could further enhance the energy imbalance.

Measurement Prospects: Resonant depolarization for transversely polarized pilot bunches together with a polarimeter is presently envisaged to determine the average beam energy, where first requirements are explored in [21, 22]. Complementary studies [8] show the possibility of measuring the boost with a precision of 50 keV per IP by analysing 10^6 dimuon events ($e^+e^- \to \mu^+\mu^-(\gamma)$), which are acquired within 5 min at the Z-pole. Interestingly, studies in [23] investigate in the design of a beamstrahlung monitor, for continuous measurements with colliding bunches.

SUMMARY AND OUTLOOK

The FCC-ee aims at performing high precision physics experiments and thus demands a precise knowledge of the ECM and boosts at all four IPs, where first results for the Z- and the tt̄-pole are presented here. Synchrotron radiation losses lead to a non-constant beam energy, and beamstrahlung at the IP enhances this asymmetry further. Nevertheless, in the case of the Z-pole with one RF-section, the ECM is almost identical at the four IPs. At the tt̄-pole with two RF-sections, the ECM and boosts strongly depend on their placement. Placing them in PH and PL introduces a systematic asymmetry between the ECM within the range of about 200 MeV, which is so far considered to be acceptable for physics requirements. The ECM and boosts will also need to be evaluated for the W- and the ZH-pole.

ACKNOWLEDGMENTS

We would like to thank the FCC energy polarization, calibration and monochromatization (EPOL) working group, O. Brunner, R. de Maria, I. Karpov and F. Peauger for fruitful discussions.

ISBN: 978-3-95450-227-1 ISSN: 2673-5490 doi:10.18429/JACoW-IPAC2022-WEPOST007

REFERENCES

[1] O. Brüning *et al.*, "LHC Design Report", CERN, Geneva, Switzerland, Rep. No. CERN-2004-003-V-1, 2004.

[2] G. Apollinari, I. Béjar Alonso, O. Brüning, P. Fessia, M. Lamont, L. Rossi and L. Tavian (eds.), "High Luminosity Large Hadron Collider (HL-LHC): Technical Design Report V.0.1", CERN Yellow Reports: Monographs, Rep. No. CERN-2017-007-M, 2017.

[3] M. Benedikt, A. Blondel, P. Janot, M. Mangano, and F. Zimmermann, "Future circular colliders succeeding the LHC", *Nature Phys.*, vol. 16, pp. 402–407, 2020.

[4] M. Benedikt *et al.* (eds.), "Future Circular Collider study, Volume 2: The Lepton Collider (FCC-ee) Conceptual Design Report", *Eur. Phys. J. ST.*, vol. 228, pp. 261 – 623, 2019.

[5] M. Benedikt *et al.* (eds.), "Future Circular Collider study, Volume 3: The Hadron Collider (FCC-hh) Conceptual Design Report", *Eur. Phys. J. ST.*, vol. 228, pp. 755–1107, 2019.

[6] K. Oide, "Status of the FCC-ee optics and next steps", presented at the FCCIS-WP2 Workshop 2021. `http://indico.cern.ch/event/1085318/`

[7] J. Gutleber, Private communication, January 2022.

[8] A. Blondel *et al.*, "Polarization and Centre-of-mass Energy Calibration at FCC-ee", 2019. `arXiv:1909.12245`

[9] Energy calibration and polarization working group `http://indico.cern.ch/category/8678`

[10] H. Wiedemann, "Particle accelerator physics", 4th edition, Springer International Publishing, 2015.

[11] MAD-X, Methodical Accelerator Design. `http://mad.web.cern.ch/mad`

[12] F.C. Iselin, "The MAD programm, physical methods manual", CERN, Geneva, Switzerland, 1994.

[13] T. H. B. Persson, H. Burkhardt, L. Deniau, A. Latina, and P. K. Skowro, "MAD-X for Future Accelerators", in *Proc. IPAC'21*, Campinas, Brazil, May 2021, pp. 2664–2667. `doi:10.18429/JACoW-IPAC2021-WEPAB028`

[14] L. van Riesen-Haupt, H. Burkhardt, T. H. B. Persson, and R. Tomás García, "Comparison of Accelerator Codes for Simulation of Lepton Colliders", in *Proc. IPAC'21*, Campinas, Brazil, May 2021, pp. 1334–1337. `doi:10.18429/JACoW-IPAC2021-TUPAB004`

[15] K. Ohmi and F. Zimmermann, "FCC-ee/CepC Beam-beam Simulations with Beamstrahlung", in *Proc. IPAC'14*, Dresden, Germany, Jun. 2014, pp. 3766–3769. `doi:10.18429/JACoW-IPAC2014-THPRI004`

[16] D. Shatilov, "Beam-beam simulations at large amplitudes and lifetime determination", *Part. Accel.*, vol. 52, pp. 65–93, 1996.

[17] S.A. Nikitin, "Formulae for estimating average particle energy loss due to beamstrahlung in supercolliders", 2020. `arXiv:2002.01173`

[18] M.A. Valdivia Garcia and F. Zimmermann, "Beam blow up due to beamstrahlung in circular e^+e^- colliders", *Eur. Phys. J. Plus*, vol. 136, p. 501, 2021.

[19] P. Janot, Private communication, 2022.

[20] F. Peauger and O. Brunner, "RF strategy for Higgs Operation", presented at the 151st FCC-ee Optics Design Meeting, 17th March 2022. `http://indico.cern.ch/event/1118299/`

[21] J. Wenninger and M. Hofer, "Polarimeter installation requirements and possibilities", presented at the EPOL Meeting, 22nd January 2022. `http://indico.cern.ch/event/1108961/`

[22] N. Muchnoi, "More on polarimeter precision and sensitivity to spurious light transverse polarization", presented at the EPOL Meeting, 17th March 2022. `http://indico.cern.ch/event/1135626/`

[23] A. Ciarma, "IP generated radiation monitor for center-of-mass energy measurements", presented at the FCC Physics Workshop 2022. `http://indico.cern.ch/event/1066234/`